Electronic Structure of TDAE−C_{60} Complex

Shojun Hino*

Department of Image Science, Faculty of Engineering, Graduate School of Science and Technology, Chiba University, Inage-ku, Chiba 263, Japan

Kazunori Umishita

Graduate School of Science and Technology, Chiba University, Inage-ku, Chiba 263, Japan

Kentaro Iwasaki

Department of Image Science, Faculty of Engineering, Chiba University, Inage-ku, Chiba 263, Japan

Kazuyoshi Tanaka, Tohru Sato, and Tokio Yamabe

Department of Molecular Engineering, Graduate School of Engineering, Kyoto University, Sakyo-ku, Kyoto 606-01, Japan

Kazunari Yoshizawa and Kenji Okahara

Institute for Fundamental Chemistry, 34-4 Nishihiraki-cho, Takano, Sakyo-ku, Kyoto 606, Japan

Received: January 13, 1997; In Final Form: March 20, 1997[⊗]

Ultraviolet and C 1s and N 1s X-ray photoelectron spectra of a ferromagnetic charge-transfer complex, TDAE−C_{60}, where TDAE is tetrakis(dimethylamino)ethylene, have been measured. The appearance of a new peak above the highest occupied band of C_{60} at 1.2 eV below the Fermi level with a peak onset of 0.5 eV indicates that an electron is transferred from TDAE to C_{60} and that TDAE−C_{60} is not metallic but semiconductive. The N 1s core spectrum of the complex shows a wide band consisting of two components, and the intensity of the higher binding energy one decreases under X-ray irradiation. The observed components could be ascribed to nitrogen atoms in $TDAE^0$ and $TDAE^{2+}$ on the basis of the electrostatic potential model in combination with the CNDO/2 molecular orbital calculation. Possible appearance of the charge density wave state along the TDAE chain in the *c*-direction of TDAE−C_{60} crystal has been suggested.

Introduction

Since the observation of *soft* ferromagnetism below 16.1 K[1] in a charge-transfer complex TDAE−C_{60}, where TDAE is tetrakis(dimethylamino)ethylene, there have been many experimental studies on its magnetic properties[2−13] as well as theoretical clarification.[14−22] X-ray diffraction measurement of TDAE−C_{60} has shown that the crystal lattice is *c*-centered monoclinic and its composition is stoichiometric with a 1:1 ratio of TDAE to C_{60}.[23] Although several mechanisms of the magnetic ordering in TDAE−C_{60} have been proposed, they are still controversial.[11] For instance, it has been discussed that the ground state of this compound is itinerant ferromagnetic,[1] superparamagnetic,[3] spin-glass-like,[24] or weak ferromagnetic.[7]

The origin of ferromagnetic behavior of TDAE−C_{60} has been ascribed to an electronic spin localized on C_{60}^-, and the effective exchange interaction between these spins has been estimated to be 5.03×10^{-4} eV by means of electron spin resonance (ESR) and Faraday-balance magnetization measurements.[8,25,26] On the other hand, since TDAE in the TDAE−C_{60} solid exhibits no signal on the ESR spectrum, information of the electronic structure of TDAE in the TDAE−C_{60} solid is limited, though the presence of TDAE cation radical in its benzonitrile solution has been confirmed by the ESR spectrum.[27] The fact that the X-band ESR study of TDAE−C_{60} solid has shown only C_{60}^- signal without TDAE signal[25] can be interpreted as there is a certain spin cancellation mechanism such as occurrence of spin density wave (SDW) or charge separation due to charge density wave (CDW) leading to $TDAE^0$ and $TDAE^{2+}$. However, Raman spectroscopy of TDAE−C_{60} and TDAE−C_{70} has shown the presence of TDAE monocation.[28,29] Recent Q-band ESR measurements by Gotschy and co-workers has suggested that C_{60}^- and $TDAE^+$ spins are strongly coupled.[13,30] These conflicting experimental results seem to be an indication that TDAE radical cation should play a certain important role in the magnetism of the TDAE−C_{60} solid. An investigation of the electronic structure of TDAE−C_{60} complex is required to have an accurate knowledge of its magnetism.

Photoelectron spectroscopy is a powerful tool to determine the electronic structure of TDAE−C_{60}. In this paper, we report the ultraviolet photoelectron spectra (UPS) of the TDAE−C_{60} complex and describe the electronic structural change near the Fermi level upon complex formation. C 1s and N 1s X-ray photoelectron spectra (XPS) are also presented and the oxidization state of TDAE in the complex is discussed with the aid of CNDO/2 calculations.

Experimental Section

High purity C_{60} (99.9 %) was purchased from Vacuum Metallurgical Co., Ltd. and TDAE from Tokyo Chemical Industry Co., Ltd. They were employed for the synthesis without further purification. The TDAE−C_{60} complex was prepared by a similar recipe to that described in ref 3; C_{60} was dissolved in the benzene−toluene (1:1) solvent, and the solution

---

* To whom correspondence should be addressed.

[⊗] Abstract published in *Advance ACS Abstracts,* May 15, 1997.

S1089-5639(97)00192-8 CCC: $14.00

was degassed by freeze and thaw cycles *in vacuo* until no further degassing was observed. TDAE was added in large excess into the solution under nitrogen gas flow for the prevention of the penetration of the ambient atmosphere, since TDAE is easily oxidized by the air and the complex is air sensitive. The TDAE−C_{60} complex was obtained as a black precipitate. The solvent and unreacted TDAE were removed by evacuation. Excellent reproducibility of the magnetic properties of the thus prepared TDAE−C_{60} sample has been observed in previous works.[25,26,31]

The samples for the ordinary photoemission measurements are prepared by vacuum deposition or by crystal cleavage, because the cleanliness of the surface is crucial. However, these methods could not be applied to TDAE−C_{60}, since its chemical composition could be affected by vacuum deposition and large crystals suitable for cleavage could not be obtained. Therefore, the samples for the measurements were crushed TDAE−C_{60} powder films prepared on an Au substrate. This procedure was carried out in an Ar-filled glovebox connected to a photoelectron spectrometer KRATOS XSAM 800 so that the sample was free from the effect of the ambient atmosphere. The photoelectron spectrometer was equipped with a helium dc discharged lamp ($h\nu = 21.2$ eV) and a Mg anode X-ray gun ($h\nu = 1253.6$ eV). The pressure of the spectrometer during the measurement was kept to 5×10^{-9} Torr or less. The energy calibration of the spectrometer for the UPS measurement was carried out by the Fermi edge of the Au evaporated film, and the peak position of the Au $4f_{7/2}$ (=84.0 eV) was used for the XPS measurement. Energy resolution of the spectrometer for the UPS measurements was estimated to be 300 meV from the width of the Au Fermi edge and that for the XPS was about 1 eV from the full width at half maximum (fwhm) of the Au $4f_{7/2}$ peak. Details of the photoelectron measurements are described elsewhere.[32,33] All the spectra were recorded at room temperature.

Results and Discussion

A. UPS. Figure 1 shows the UPS of TDAE-C_{60}. The UPS of C_{60} evaporated film (solid line) and powder C_{60} sample (broken line) are also shown for comparison. Five structures labeled **A**−**E** are observed in the spectrum of TDAE−C_{60}, and the corresponding structures are also observed in the spectra of C_{60}. There are, however, several different points among these spectra. In the spectrum of TDAE−C_{60}, the deeper the binding energy (lower kinetic energy), the stronger the intensity, which is not observed in the spectrum of the C_{60}-evaporated film and is slightly observed in that of the powder C_{60} sample. This effect might be due to the electron scattering in the sample film, since an enhancement of the lower kinetic energy region in the UPS is a typical phenomenon when the specimen is contaminated. The reason why the amounts of the low-kinetic-energy scattered secondary electrons were larger in the powder C_{60} specimen than those in the evaporated film could be due to the difference in degree of surface cleanness between the two samples. While C_{60} used for the photoelectron measurements was sublimed at least once, TDAE−C_{60} did not experience sublimation after the preparation. It is plausible that surface of the TDAE−C_{60} powder sample is more contaminated than the other two, since nonvolatile impurities derived from the solvent could not be removed from the specimen.

There is an additional structure labeled **N** in the spectrum of TDAE−C_{60} just below the Fermi level that is not observed in C_{60} (see inset). It is located at 1.2 eV below the Fermi level with a peak onset of 0.5 eV in the complex spectrum. A clear gap between the Fermi level and the spectral onset is an indication that TDAE−C_{60} solid is not metallic but semiconductive. The small onset energy of the TDAE−C_{60} complex compared with C_{60} (1.9 eV[34,35]) is related to its higher electric conductivity (10^{-4} S cm^{-1} at room temperature; ref 36) than that of C_{60} itself (~10^{-8} S cm^{-1} or less depending on the quality, ref 37). The appearance of a new peak in the vicinity of the Fermi level has also been observed in the course of successive alkali metal dosing to C_{60} and fullerenes.[34,35,38−40] Since TDAE is a strong electron donor, the new peak must be a result of the electron transfer from the highest occupied molecular orbital (HOMO) of TDAE to the lowest unoccupied molecular orbital (LUMO) of C_{60}. The intensity ratio of **N** to **A** is about 1:10. From analogy of the spectral change upon alkali metal dosing[34,35,38−40] and from the result of the elemental analysis of the complex,[1,3] the amount of electron transferred from TDAE to C_{60} can be counted as unity per TDAE−C_{60} pair. This result is consistent with the estimation of spin concentration of approximately one spin per C_{60} molecule from the Faraday-balance magnetization measurement.[3,25]

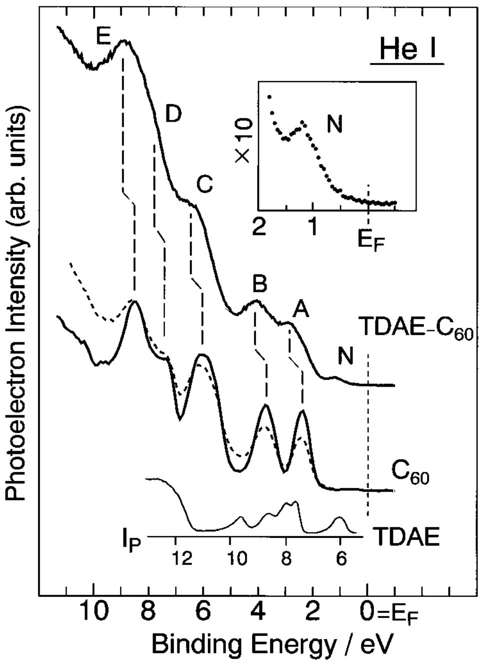

Figure 1. An ultraviolet photoelectron spectrum of the TDAE−C_{60} complex. The spectra of a C_{60}-evaporated film (solid line) and a C_{60} powder sample (broken line) and gaseous TDAE[41] are also shown for comparison. The intensity of the spectra of C_{60} and TDAE are adjusted so as to reflect their number of electrons occupied in their MOs. The spectrum of TDAE is shifted by 5 eV, which is an averaged energy difference between gas and solid phase photoelectron spectra.[42] An expanded spectrum of TDAE−C_{60} just below the Fermi level is shown in the inset.

All the spectral structures of TDAE−C_{60} are shifted by *ca.* 0.5 eV uniformly toward the higher binding energy side than those of C_{60} spectra. An analogous shift has been observed at the first stage of alkali metal dosing to fullerenes, and it was interpreted in terms of the shift of the Fermi level.[34,35,38−40] The origin of the observed shift might also be the change of the Fermi level upon the complex formation, since the low-kinetic-energy cutoff of the spectrum is also shifted by the same amount.

The width of each structure in the TDAE−C_{60} spectrum is much broader than that in the C_{60} spectrum. This broadening is typical to structures A and B. The broadening could be either due to superposition of the spectrum of TDAE to that of C_{60} or to the result of an interaction between C_{60} and TDAE, besides the electron scattering induced by the contamination of the

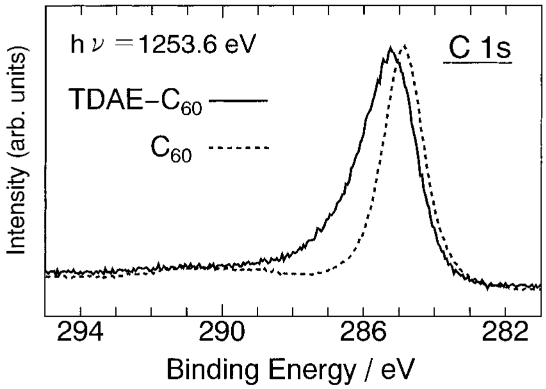

Figure 2. C 1s spectra of TDAE$-$C$_{60}$ (solid line) and C$_{60}$ powder (broken line). Note that the spectrum of the complex is broad and shifted toward the higher binding energy side.

specimen. Contribution from TDAE as well should be taken into account as well for consideration of the TDAE$-$C$_{60}$ spectrum. Gas phase UPS and TDAE[41] is shown in Figure 1 for comparison. As it is referred to the vacuum level, the energy scale of the spectrum is shifted by 5 eV, which is an averaged amount often adopted in comparison between the gas and solid phase spectra.[42] The intensity of the TDAE spectrum is adjusted to reflect the numbers of the electrons in TDAE and C$_{60}$; the first bands of the TDAE and C$_{60}$ spectra consisted of 2 and 10 electrons, respectively. It seems that the contribution from TDAE itself to the spectrum of TDAE$-$C$_{60}$ is small in the low-binding energy region, since the number of the TDAE electrons in this region is smaller than that of the corresponding electrons of C$_{60}$. Therefore the broadening derives mainly from the interaction between C$_{60}$ and TDAE. Upon complex formation, Jahn$-$Teller effect takes place and the C$_{60}$ MO levels are spread to form wide bands.[43,44] Charge transfer from TDAE to C$_{60}$ induces Coulombic forces among the constituent molecules, and the carbon atoms in C$_{60}$ might feel different Madelung potential. These effects could cause the broadening of the peaks.

B. C 1s XPS. Figure 2 shows the C 1s core spectrum of TDAE$-$C$_{60}$. The spectral shape did not change in the course of the XPS measurements so that the C 1s core level was believed to have suffered no serious damage from the X-ray irradiation. For comparison, the spectrum obtained from the C$_{60}$ powder sample (broken line) is also shown. The C 1s peak of TDAE$-$C$_{60}$ is located at 285.1 eV with 1.9 eV fwhm. The peak position shifts toward the higher binding energy side, and the peak profile is asymmetric compared with that of C$_{60}$. This shift corresponds to what is observed in UPS. There are two possible reasons for the origin of the peak asymmetry: one is the superposition of the photoelectrons from TDAE. The binding energy of 10 carbon atoms in the TDAE molecules might be larger than that of C$_{60}$, since TDAE is electron deficient due to the electron transfer from TDAE to C$_{60}$. Another reason is the shake-up effect. Because of the formation of the band N in the band gap of pristine C$_{60}$ (about 2 eV, ref 45), the band gap of the complex is believed to become around 0.5 eV (corresponding to the onset energy of structure **N**). As the narrow band gap is in favor of producing the secondary electrons of which kinetic energy is slightly smaller than that of the photoelectrons main peak, shake-up-induced peak asymmetry (Doniach$-$Sunjic type deformation[46]) could take place in the complex, and the C 1s peak profile was skewed to the higher binding energy side.

C. N 1s XPS. Figure 3 shows the N 1s core spectra of the TDAE$-$C$_{60}$ complex. The spectrum a was measured with 3 h accumulation from just after the introduction of the sample into the spectrometer. The spectrum b was a result of data acquisition in the successive three hours after the measurement of spectrum a. Both spectra consist of a main peak and a satellite peak labeled S. The main peak can be deconvoluted into two peak components labeled A and B located at 399.8 and 401.3 eV, respectively. Note that the splitting between them is 1.5 eV and that component B is due to less negatively charged nitrogen atoms than component A. The origin of this splitting must be the chemical shift induced by the electron transfer from the nitrogen atoms to C$_{60}$ molecules. A result of peak profile analysis is also shown in Figure 3, where numerics indicate the intensity ratio of the three structures assuming the intensity of component A to be 100. Since the spectra are the time-averaged ones, the spectrum obtained at the first scan may be different from that shown in Figure 3 with high probability.

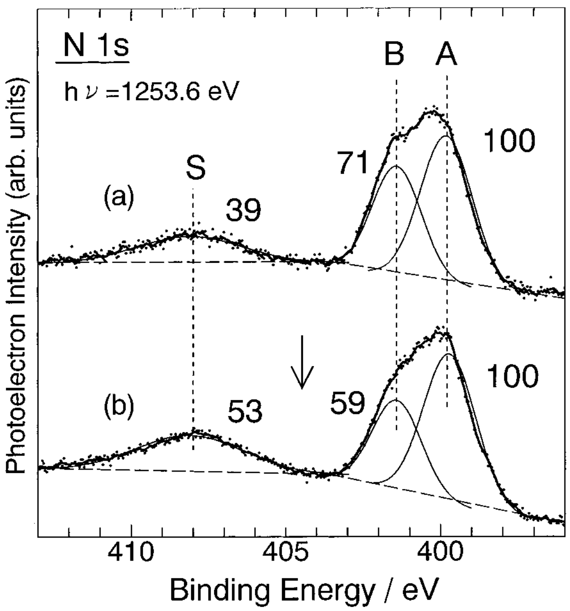

Figure 3. N 1s core spectra of TDAE$-$C$_{60}$ complex. The spectrum a was accumulated for 3 h from just after the introduction of the sample into the spectrometer, and the spectrum b was acquisited for 3 h after the measurement of spectrum a. Two peak components and a satellite are observed. Numerics in the figure indicate the intensity ratio obtained by a peak profile analysis of the three structures. (The intensity of component A is assumed to be 100.)

In the course of measurements, the intensity of component B decreases and that of satellite S increases, although these phenomena were not observed in the sample that was kept in the spectrometer without X-ray irradiation. Therefore, the change in the intensity can be concluded to be the result of X-ray irradiation itself. Their integrated intensity hardly changes, although the intensity of components A and B changes. Since the amount of decrease and increase are complementary, component B and satellite S derive from the same origin and component A comes from a different one. Therefore, the spectrum of an as-prepared fresh sample have probably only two main peak components of nearly the same intensity with a possible very small satellite peak. This inference and the argument in UPS section lead to two possible electronic structures of the nitrogen atoms in the complex: (A) co-existence of two neutral and two negatively charged nitrogen atoms in the TDAE^{+} state or (B) existence of equal amounts of TDAE^{0} of four equivalent neutral nitrogen atoms and TDAE^{2+} of four equivalent negatively charged nitrogen atoms.

D. CNDO/2 Calculation. The chemical shift from the netural state observed in XPS can be calculated using the conventional electrostatic potential model[47] based on the equilibrium molecular geometries. According to this model, chemi-

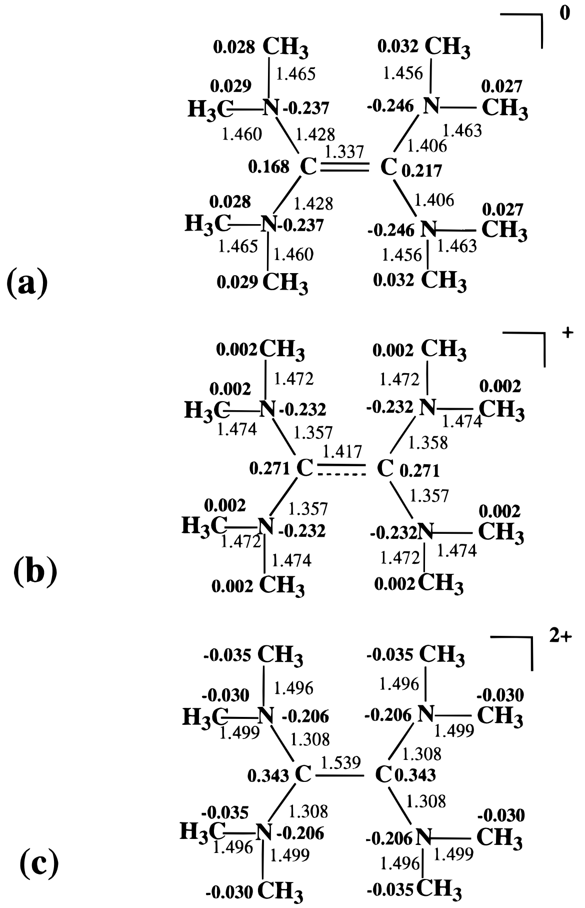

Figure 4. CNDO/2 atomic net charges at the equilibrium geometries[29] of (a) $TDAE^0$, (b) $TDAE^+$, and (c) $TDAE^{2+}$. The CNDO charge is denoted by bold letters, and the bond length in angstroms by plain ones. These geometries have been obtained by the *ab initio* MO calculation (HF/3-21G level). Note that all of these molecules are not planar, and asymmetric charge distribution in (a) is due to its asymmetric equilibrium geometry.

cal shift $\Delta E(\mathrm{A})$ of atom A is given by

$$\Delta E(\mathrm{A}) = kq_A + \sum_{B \neq A} \frac{e^2 q_B}{R_{AB}} + 1 \qquad (1)$$

where q_A or q_B is formal charge on the atom A or B, respectively, R_{AB} is interatomic distance, and k and l are parameters specified to atom A. It has been confirmed that the value thus estimated is in good agreement with the experimentally observed shift with a few exceptions.[47] We employ $k = 21.5$ eV/(unit charge) and $l = -1.7$ eV as parameters of nitrogen.[47] The equilibrium molecular geometries obtained with *ab initio* MO calculation[29] are used for the calculation (bond lengths are shown by plain letters in Figure 4).

Estimated atomic net charges of $TDAE^0$, $TDAE^+$, and $TDAE^{2+}$ with the semi-empirical CNDO/2 method are shown in Figure 4 (boldface letters). Because of a short distance between the two vinyl carbons and large repulsion among methyl groups attached to the nitrogen atoms, $TDAE^0$ is nonplanar and asymmetric and has two pairs of two sets of equivalent nitrogen atoms with −0.246 and −0.237 charges. On the other hand, all four nitrogen atoms in $TDAE^+$ and $TDAE^{2+}$ have equivalent −0.232 and −0.206 charges, respectively. Equation 1 with consideration of only the first nearest-neighbor atoms of the nitrogen atoms, that is, vinyl carbons and carbon atoms of methyl group, gives following chemical shifts from the neutral state of N 1s: $\Delta E = -4.2$ and -4.6 eV for the two equivalent nitrogen atoms in $TDAE^0$, $\Delta E = -3.8$ eV for $TDAE^+$, and $\Delta E = -3.0$ eV for $TDAE^{2+}$. If the origin of the two peak components observed in the N 1s spectra belongs to $TDAE^0$, the difference in their calculated chemical shifts (0.4 eV) is far smaller than that between the experimental ones, and the two components should have decreased equally by the X-ray irradiation because there are few differences in the bonding conditions of the nitrogen atoms in $TDAE^0$ (see Figure 4).

When the chemical shifts in $TDAE^0$ are averaged to be −4.4 eV, the difference in the calculated chemical shift between $TDAE^0$ and $TDAE^+$ is 0.6 eV and that between $TDAE^0$ and $TDAE^{2+}$ is 1.4 eV. The amount of the observed splitting in components A and B and their intensity indicate coexistence of the same amounts of $TDAE^0$ and $TDAE^{2+}$ in the complex rather than the presence of $TDAE^+$ with unreacted $TDAE^0$. This deduction is consistent with the gradual increase of the satellite S upon X-ray irradiation and is also supported by the charge disproportionation in TDAE. The optimized C═C bond lengths are 1.337, 1.417, and 1.539 Å for $TDAE^0$, $TDAE^+$, and $TDAE^{2+}$, respectively, as shown in Figure 4.[29] That is, removal of the electron from $TDAE^0$ (ionization) lengthens the C═C bond. As the HOMO of $TDAE^0$ mainly consists of a π-bonding orbital on the vinyl carbons, ionization could weaken the C═C bond. The increase of satellite S might be the result of decomposition of $TDAE^{2+}$ by the X-ray irradiation, because the lengthened and possibly weakened C═C bond in $TDAE^{2+}$ may be vulnerable to the X-ray damage compared with those in $TDAE^0$ and $TDAE^+$. As for the charge disproportionation, the first and the second half-wave potentials of TDAE *vs* saturated calomel electrode are close each other to be −0.75 and −0.61 V, respectively.[48] As this reaction has been observed in the benzonitrile solution of TDAE−C_{60},[27] an analogous charge separation reaction, $TDAE^+ + TDAE^+ \rightarrow TDAE^0 + TDAE^{2+}$ may easily take place in the complex.

Recent X-ray diffraction measurement[7] has shown that the unit-cell size in the *c*-direction is twice as large as that reported previously[23] and that each TDAE molecule shifts toward opposite direction along the *b*-axis by *ca*. 0.02 Å. This crystal structure is consistent with the charge disproportionation. Possibly the C═C bonds in the TDAE molecules are arranged to have a kind of chain structure in the *c*-direction of the crystal so as to form the CDW state along it.

Conclusions

Ultraviolet and X-ray photoelectron spectra of a charge-transfer complex TDAE−C_{60} have been observed. Results and discussion on the electronic structure including the oxidization state of nitrogen in the complex leads to four major findings. (1) The appearance of a new peak at 1.2 eV below the Fermi level with the peak onset of 0.5 eV in the UPS spectrum above the highest occupied band of C_{60} indicates one electron transfer from TDAE to C_{60} and semiconductive nature of the complex. (2) An uniform peak shift of *ca*. 0.5 eV toward the higher binding energy side is observed in the spectra of TDAE−C_{60}, which is similar to the first stage of alkali-metal dosing to C_{60} and is ascribed to the shift of the Fermi level on complexation. (3) The C 1s core band is broad and asymmetric. The N 1s core spectrum is a wide band consisting of two components and the intensity of the higher energy one decreases under X-ray irradiation, which indicates two oxidation states in the complex. (4) Two oxidation states of the complex is examined by the CNDO/2 level electrostatic potential calculation, and they can be interpreted by coexistence of $TDAE^0$ and $TDAE^{2+}$ rather than $TDAE^+$ alone. This suggests an appearance of the charge density wave along the *c*-direction of the TDAE-C_{60} crystal.

Acknowledgment. This work was supported by a Grant-in-Aid for Scientific Research (Grant 05233110) from the Ministry and Education, Science and Culture of Japan, Research fund of Graduate School of Science and Technology, Chiba University, and also was partially funded by Research for the Future program of the Japan Society for the Promotion of Science (Project JSPS-RFTF96P00206). TS is grateful to the Research Fellowships of the JSPS for Young Scientists for financial support. Numerical calculations were carried out at the Data Processing Center of Kyoto University and the Supercomputer Laboratory of the Institute for Chemical Research of Kyoto University.

References and Notes

(1) Allemand, P.-M.; Khemani, K. C.; Koch, A.; Wudl, F.; Holczer, K.; Donovan, S.; Grüner, G.; Thompson, J. D. *Science* **1991**, *253*, 301.

(2) Sparn, G.; Thompson, J.; Allemand, P.-M.; Li, Q.; Wudl, F.; Holczer, K.; Stephens, P. *Solid State Commun.* **1992**, *82*, 779.

(3) Tanaka, K.; Zakhidov, A. A.; Yoshizawa, K.; Okahara, K.; Yamabe, T.; Yakushi, K.; Kikuchi, K.; Suzuki, S.; Ikemoto, I.; Achiba, Y. *Phys. Rev. B* **1993**, *47*, 7554.

(4) Suzuki, A.; Suzuki, T.; Whitehead, R. J.; Maruyama, Y. *Chem. Phys. Lett.* **1994**, *223*, 517.

(5) Mihailovic, D.; Lutar, K.; Hassanien, A.; Cevc, P.; Venturini, P. *Solid State Commun.* **1994**, *89*, 209.

(6) Blinc, R.; Cevc, P.; Arcon, D.; Mihailovic, D.; Venturini, P. *Phys. Rev. B* **1994**, *50*, 13051.

(7) Blinc, R.; Pokhodnia, K.; Cevc, P.; Arcon, D.; Omerzu, A.; Mihailovic, D.; Venturini, P.; Golivc, L.; Trontelj, Z.; Luvznik, J.; Jeglivcivc, Z.; Pirnat, J. *Phys. Rev. Lett.* **1996**, *76*, 523.

(8) Tanaka, K.; Sato, T.; Yamabe, T.; Yoshizawa, K.; Okahara, K.; Zakhidov, A. A. *Phys. Rev. B* **1995**, *51*, 990.

(9) Tanaka, K.; Sato, T.; Yoshizawa, K.; Okahara, K.; Yamabe, T.; Tokumoto, M. *Chem. Phys. Lett.* **1995**, *237*, 123.

(10) Tokumoto, M.; Song, Y. S.; Tanaka, K.; Sato, T.; Yamabe, T. *Solid State Commun.* **1996**, *97*, 349.

(11) Mihailovic, D.; Arcon, D.; Venturini, P.; Blinc, R.; Omerzu, A.; Cevc, P. *Science* **1995**, *268*, 400.

(12) Lappas, A.; Prassides, K.; Vavekis, K.; Arcon, D.; Blinc, R.; Cevc, P.; Amato, A.; Feyerherm, R.; Gygax, F. N.; Schenck, A. *Science* **1995**, *267*, 1799.

(13) Gotschy, B. *Phys. Rev. B* **1995**, *52*, 7378.

(14) Yamaguchi, K.; Hayashi, S.; Okamura, M.; Nakano, M.; Mori, W. *Chem. Phys. Lett.* **1994**, *226*, 372.

(15) Arovas, D.; Auerbach, A. *Phys. Rev. B* **1995**, *52*, 10114.

(16) Tanaka, K.; Asai, Y.; Sato, T.; Kuga, T.; Yamabe, T.; Tokumoto, M. *Chem. Phys. Lett.* **1996**, *259*, 574.

(17) Asai, Y.; Tokumoto, M.; Tanaka, K.; Sato, T.; Yamabe, T. *Phys. Rev. B* **1996**, *53*, 4176.

(18) Kawamoto, T. *Solid State Commun.* In press.

(19) Sato, T.; Yamabe, T.; Tanaka, K. *Phys. Rev. B.* submitted for publication

(20) Sato, T.; Saito, T.; Yamabe, T.; Tanaka, K.; Kobayashi, H. *Phys. Rev. B.* In press.

(21) Sato, T.; Tanaka, K.; Saito, T.; Yamabe, T. *Proceedings of the 11th General Symposium on Fullerenes*; Aug 2−3, 1996; Sapporo, Japan; Fullerene Research Association, Department of Knowledge-Based Information Engineering, Toyohashi University of Engineering: Toyohashi, Japan 1996.

(22) Sato, T.; Yamabe, T.; Tanaka, K. *Proceedings of the 12th General Symposium on Fullerenes*; Jan 13−14, 1997, Tokyo, Japan; Fullerene Research Association, Department of Knowledge-Based Information Engineering, Toyohashi University of Engineering: Toyohashi, Japan 1997.

(23) Stephens, P. W.; Cox, D.; Lauher, J. W.; Mihaly, L.; Wiley, J.; Allemand, P.-M.; Hirsch, A.; Holczer, K.; Li, Q.; Thompson, J. D.; Wudl, F. *Nature* **1992**, *355*, 331.

(24) Cevc, P.; Blinc, R.; Erzen, V.; Arcon, D.; Zalar, B.; Mihailovic, D.; Venturini, P. *Solid State Commun.* **1994**, *90*, 543.

(25) Tanaka, K.; Zakhidov, A. A.; Yoshizawa, K.; Okahara, K.; Yamabe, T.; Yakushi, K.; Kikuchi, K.; Suzuki, S.; Ikemoto, I.; Achiba, Y. *Phys. Lett. A* **1992**, *164*, 221.

(26) Tanaka, K.; Yoshizawa, K.; Sato, T.; Yamabe, T.; Okahara, K.; Zakhidov, A. A. *Solid State Commun.* **1993**, *87*, 1055.

(27) Yoshizawa, K.; Sato, T.; Tanaka, K.; Yamabe, T.; Okahara, K. *Chem. Phys. Lett.* **1993**, *213*, 498.

(28) Denisov, V.; Zakhidov, A. A.; Ruani, G.; Zamboni, R.; Taliani, C.; Tanaka, K.; Yoshizawa, K.; Okahara, K.; Yamabe, T. *Synth. Met.* **1993**, *56*, 3050.

(29) Tanaka, K.; Sato, T.; Yamabe, T. *J. Phys. Chem.* **1996**, *100*, 3980.

(30) Gotschy, B.; Gompper, R.; Klos, H.; Schilder, A.; Schuts, W.; Volkel, G. *Synth. Met.* **1996**, *77*, 287.

(31) Tanaka, K.; Tanaka, T.; Atake, T.; Yoshizawa, K.; Okahara, K.; Sato, T.; Yamabe, T. *Chem. Phys. Lett.* **1994**, *230*, 271.

(32) Hino, S.; Matsumoto, K.; Yamakado, H.; Yakushi, K.; Kuroda, H. *Synth. Met.* **1989**, *32*, 301.

(33) Hino, S.; Iwasaki, K.; Tatematsu, H.; Matsumoto, K. *Bull. Chem. Soc. Jpn.* **1990**, *63*, 2199.

(34) Wertheim, G. K.; Buchanan, D. N. E. *Phys. Rev. B* **1993**, *47*, 12912.

(35) Morikawa, T.; Takahashi, T. *Solid State Commun.* **1993**, *87*, 1017.

(36) Schilder, A.; Klos, H.; Rystau, I.; Schütz, W.; Gotschy, B.; *Phys. Rev. Lett.* **1994**, *73*, 1299.

(37) Arai, T.; Murakami, Y.; Suematsu, H.; Kikuchi, K.; Achiba, Y.; Ikemoto, I. *Solid State Commun.* **1992**, *84*, 827.

(38) Hino, S.; Matsumoto, K.; Hasegawa, S.; Kamiya, K.; Inokuchi, H.; Morikawa, T.; Takahashi, T.; Seki, K.; Kikuchi, K.; Suzuki, S.; Ikemoto, I.; Achiba, Y. *Chem. Phys. Lett.* **1992**, *190*, 169.

(39) Hino, S.; Matsumoto, K.; Hasegawa, S.; Inokuchi, H.; Morikawa, T.; Takahashi, T.; Seki, K.; Kikuchi, K.; Suzuki, S.; Ikemoto, I.; Achiba, Y. *Chem. Phys. Lett.* **1992**, *197*, 38.

(40) Hino, S.; Matsumoto, K.; Hasegawa, S.; Iwasaki, K.; Yakushi, K.; Morikawa, T.; Takahashi, T.; Seki, K.; Kikuchi, K.; Suzuki, S.; Ikemoto, I.; Achiba, Y. *Phys. Rev. B* **1993**, *48*, 8418.

(41) Cetinkaya, B.; King, G. H.; Krishunamurthy, S. S. Lappert, M. F.; Pedley, J. B. *Chem. Commun.* **1971**, 1370.

(42) Grobman, W. D.; Koch, E. E. Photoemission in Solids II; Ley, L., Cardona, M., Eds.; Springer-Verlag: Berlin, 1979.

(43) Tanaka, K.; Okada, M.; Okahara, K.; Yamabe, T. *Chem. Phys. Lett.* **1992**, *193*, 101.

(44) Koga, N.; Morokuma, K. *Chem. Phys. Lett.* **1992**, *196*, 191.

(45) Dresselhaus, M. S.; Dresselhaus, G.; Eklund, P. C. *Science of Fullerenes and Carbon Nanotubes*; Academic Press: San Diego, 1996.

(46) Doniach, S.; Sunjic, M. *J. Phys. C* **1970**, *3*, 285.

(47) Siegbahn, K.; Nordling, C.; Johansson, G.; Hedman, J.; Heden, P.; Hamrin, K.; Gelius, U.; Bergmark, T.; Werme, L. O.; Manne, R.; Baer, Y. ESCA: Applied to Free Molecules; North-Holland: Amsterdam, 1969.

(48) Kuwata, K.; Geske, D. *J. Am. Chem. Soc.* **1964**, *86*, 2101.